AN EFFECTIVE BOUNDARY INTEGRAL APPROACH FOR THE SOLUTION OF NONLINEAR TRANSIENT THERMAL DIFFUSION PROBLEMS

Okey Oseloka Onyejekwe

Computational Science Program
Addis Ababa University
Arat Kilo Campus
Addis Ababa
Ethiopia

Abstract. Numerical calculations of nonlinear transient thermal diffusion problems have been carried out with a modified 'simple' boundary integral formulation known as the Green element method (GEM). The theory of the formulation is based on the singular integral equation of the boundary element method (BEM) but its implementation is element-by-element like the finite element method (FEM). Domain integrals resulting from nonlinearity of the problems as well as those arising from the approximation of the time derivative are encountered but unlike the classical approach, they are resolved within the element domain. Comparisons of GEM results with those obtained analytically or from the finite difference Newton-Richtmeyer's and the finite element method (FEM) serve to confirm the usefulness of the proposed formulation in handling nonlinearity in an unambiguous, straightforward and elegant manner without transforming or complicating the governing equations.
Keywords: nonlinearity, boundary element method, finite element method, finite difference method, Green element method, Newton-Richtmeyer, transient, thermal, diffusion.

1. Introduction

The overall conception that the boundary element method (BEM) is capable of solving many complex numerical problems in engineering and science is founded on the volumes of published work in this field that have found their way into scientific literature for the past few decades. In addition the ease with which BEM handles the aspect ratio degradation, its pointwise application of the discretized governing equation which not only facilitates its handling of high gradient scalar fields but also enhances the use of coarser grids around the vicinity of point loads and singularities, its ability to compute both the dependent variable and its flux simultaneously with the same level of accuracy, its relative ease of formulation and its boundary-only discretization which leads to a reduction in problem dimensionality are among one of those attractive features which lend the method its unique qualities. BEM superiority over other traditional numerical methods has been demonstrated in the way it handles the Laplace equation and in the solution of those nonlinear problems that are amenable to transformations of the type that enhance domain-avoidance. In all these demonstrations the full BEM coefficient matrix equation has always been put to task[1]-[9]. In as much as the relative advantages of BEM attract more and more users there are still some issues concerning its application that have not been fully addressed. For example some of the relatively simple however extremely challenging problems that are yet to be resolved include time-dependent heat diffusion problems, problems involving nonlinearity, heterogeneity, non-smooth problems. Although some of these problems have been used to validate BEM codes, the ponderous mathematical rigor involved in inventing techniques and artifices designed to contain body-force terms and deal with the problem domain have led to various types of BEM techniques [10]-[19]. Extensions to some nonlinear problems like the Navier-Stokes equations are not straightforward and are still in their elementary stages of implementation. It still remains a concern how singularity in heat flux as well as issues related to nonlinearity and heterogeneity have not been satisfactorily and straightforwardly dealt with by BEM approach. Neither is it clear why there is a noticeable scarcity of 1-D BEM codes specifically written to address 1-D type problems like in finite difference and finite element methods. As a consequence, optimism about the accuracy and advantages of BEM remain tenuous as we deal with a variety of the problems mentioned above. This is indicative BEM's restricted ability to only handle steady state problems or any problem for that matter that does not involve any numerical calculations involving the problem domain. It is worthy of note that the reason for this dramatic loss of accuracy remains unclear and has not been fully addressed in boundary element literature. Our primary aim in this paper is to further explore numerically the adaptation of the boundary integral formulation to handle nonlinearity and domain discretization [20]-[29]. The singular integral equation which results from applying the Green's second identity to the stationary part of the Laplace operator (the linear diffusion operator) is applied to the problem domain in a way that is akin to the finite element implementation. This approach though boundary integral based adopts domain discretization unreservedly and gains immensely from the finite element handling of the problem domain especially for those problems whose physics dictate an encounter with domain discretization. Past experience [1]-[5] clearly indicates that avoiding the problem domain at all costs or devising rigorous techniques to transfer all domain integrals to the boundary has not only met with mixed fortunes but in actual fact considerably slowed down the development of BEM into a highly efficient and competitive numerical tool.

2. Theoretical background

Let us consider a heat conductor with a nonlinear constitutive equation for the heat flux. The heat conduction equation to be satisfied by the temperature field for this specification is give by:

$$\frac{\partial}{\partial x}\left(D(\theta)\tfrac{\partial \theta}{\partial x}\right) = \rho c \frac{\partial \theta}{\partial t} + F(x,t,\theta) \tag{1}$$

where θ is the temperature, D, ρ and c are are the temperature dependent thermal conductivity, density and specific heat respectively and F is the heat source function. Nonlinearity of the transient-state heat conduction is contributed generally by: nonlinear boundary conditions as well as the thermal conductivity dependence on the scalar variable. Such problems have found great relevance in various areas of engineering, mathematical physics, and applied science, especially in areas such as thermo-structural design of nuclear reactors and microwave heating. The difficulties arising from the nonlinearities associated with equation (1) informed the choice of numerical technique for the solution. In boundary element applications most of the approaches adopted relies heavily on the transformation of the governing equations into corresponding analogs that help to eliminate or obfuscate all impacts of domain integrations on the solution profile. Though some of the earlier attempts in this field were beset by errors encountered in transforming from one plane of computation to the other recent improvements have resulted in encouraging results. One of the earliest attempts to deal with nonlinearity by adopting a boundary integral procedure can be found in [30-34]. Attempts to improve on this body of work can only add to the competitiveness of BEM by investigating and clarifying in a realistic way specific problems that are peculiar to BEM formulation.

2.1. The Green element formulation by linear interpolation basis functions

A unique solution to the mathematical statement expressed by equation (1) can be obtained when appropriate conditions for the dependent variable θ as well as its flux $q = -D\nabla\theta.n$ are specified on the boundary of the problem domain. There can be three of this namely: the Dirichlet-type condition specifies the temperature on the boundary:

$$\theta(x,t) = \theta_1(t) \tag{2a}$$

The heat flux can be specified across another part of the problem domain to give the Neumann-type boundary condition.

$$-D\nabla\theta.n = q_2(t) \tag{2b}$$

The Robbin or Cauchy-type boundary condition can be specified on a boundary to give:

$$\vartheta_1\theta + \vartheta_2 D\nabla\theta.n = \Psi_3(t) \tag{2c}$$

GEM formulation starts by putting equation (1) into its Poisson form:

$$\frac{\partial^2\theta}{\partial x^2} = \frac{1}{D(\theta)}\left[-\frac{\partial D}{\partial\theta}\frac{\partial\theta}{\partial x} + \rho c\frac{\partial\theta}{\partial x} + f(x,t,\theta)\right] \tag{3a}$$

or

$$\frac{\partial^2\theta}{\partial x^2} = -\frac{\partial LnD}{\partial x}\vartheta + \frac{1}{D(\theta)}\left[\frac{\partial((\beta)\theta)}{\partial t} + f\right] \tag{3b}$$

where $\beta(\theta) = \rho(\theta)c(\theta)$ is the heat capacity of the medium and $\vartheta = \partial\theta/\partial x$.

The auxiliary differential equation $\frac{d^2G}{dx^2} = \delta(x - x_1)$ as well as the Green's second identity are adopted to convert equation(1) into its integral analog:

$$\begin{aligned} &\lambda\theta(x_i, t) + G^*(x_2, t)\theta x_2, t - G^*(x_1, t)\theta(x_1, t) \\ &\quad - G(x_2, t)\vartheta(x_2, t) + G(x_1, t)\vartheta(x_1, t) \\ &\quad + \int_{x_1}^{x_2} G(x, x_1)\left[-\frac{\partial LnD}{\partial x}\vartheta(x, t) + \frac{1}{D(\theta)}\left(\beta(\theta)\frac{\partial\theta}{\partial t} + f\right)\right] dx = 0 \end{aligned} \tag{4}$$

where the subscript I denotes the source point, λ is the Cauchy integration of the Dirac delta function and is given a value of 0.5 when situated at the boundary of the problem domain otherwise it is 0.5, $G(x, x_1) = \frac{(|x - x_1| + p)}{2}$ is the Green's function and $G^*(x, x_1) = \frac{dG(x, x_i)}{dx}$ is the derivative of the Green's function. It is worthwhile to comment that equation (4) is a boundary integral formulation and applies to both the problem domain as well as its boundary. The finite element implementation of equation(4) is the core of GEM and in line with this Lagrange type interpolation function are prescribed for the dependent variable θ and its functions: $LnD(\theta)$, $\frac{1}{D(\theta)}$, $\vartheta(\theta)$. This is put in the general form:

$$\xi \approx \omega_j\xi_j \tag{5}$$

where ω_j is the interpolating function with respect to node j and the Einstein summation for the repeating index indicates summation for all the nodes in a particular element of the problem domain. Substituting the interpolation function as well as the expressions for $G(v, x_i)$ and $G^*(x, x_i)$ yields a system of discrete element equations:

$$R_{ij}\theta_j + (L_{ij} - U_{inj}\Theta_n)\vartheta_j + T_{inj}\left(\psi_n\frac{d\theta_j}{dt}\right) = 0,\ i, j, n = 1, 2 \tag{6}$$

where the discrete element matrices R_{ij},L_{ij},U_{ij}, T_{inj} have all been defined [27]. In GEM computation we propose that the problem domain be divided into a finite number of arbitrary sub-regions or elements where a continuous function is approximated by a piecewise function in such a way that at the nodes, the values of the approximating function coincide with those of the approximated function. Furthermore, the approximating functions are chosen in such a way as to satisfy the continuity requirement along the surfaces separating the adjacent elements. Given this procedure, we may look at the approximations of the scalar field within a particular element independent of what happens in adjacent or neighboring elements. It is this unique aspect of the finite element technique that enhances GEM's handling of nonlinearity and heterogeneity.

Equation (6) represents a system of nonlinear equations that describes heat conduction in an element in terms of the values of the temperature at the nodes of that element. On assembling the whole system of element equations for the entire problem domain, the node points of each element, become the interior nodes except those on the boundaries which are referred to as the boundary nodes. A finite difference approximation of the temporal derivative yields:

$$\left.\frac{d\theta_i}{dt}\right|_{t=t_{m+\alpha\Delta t}} = \frac{\theta_i^m - \theta_i^{m+1}}{\Delta t}$$

where $\Delta t = t^{(m+1)-t^m}$ and α is a time weighting factor over a range $0 \leq \alpha \leq 1$. As a result, equation (6) becomes:

$$\begin{aligned} &\left[\alpha R_{ij} + \frac{T_{inj}(\alpha\psi_n^{(m+1)} + (1-\alpha)\psi_n^m)}{\Delta t}\right]\theta_j^{m+1} + \alpha\left[L_{ij} - U_{inj}\Theta_n\right]\vartheta^{(m+1)_j} \\ &+\left[(1-\alpha)R_{ij} + \frac{T_{inj}(\alpha\psi_n^{(m+1)}+(1-\alpha)\psi_n^m)}{\Delta t}\right]\theta_j^{m+1} + (1-\alpha)[L_{ij}-U_{inj}\Theta_n]\vartheta^{(m)_j} \\ &+ T_{inj}[\alpha k_n^{m+1} + (1-\alpha)k_n^m][\alpha f_n^{(m+1)} + (1-\alpha)f_n^m] \equiv g_i = 0,\ i,j,n = 1,2. \end{aligned} \tag{7}$$

Equation (7) is a system of nonlinear element discrete equations. The Newton-Raphson technique is adopted for the linearization process to yield:

$$J_{ij}^{m+1} = \begin{cases} \left.\dfrac{\partial g_i}{\partial\theta_j}\right|_{\theta_j=\ \theta_j^{m+1}} & = \ \alpha R_{ij} + \dfrac{T_{inj}[\alpha\psi_n^{m+1} + (1-\alpha)\psi_n^m]}{\Delta t} \\ & \quad + \dfrac{\alpha T_{inj}[\alpha\theta_n^{m+1} + (1-\alpha)\theta_n^{(m)}]}{\Delta t}\dfrac{d\psi}{d\theta_j} \\ & \quad -\alpha U_{inj}\varphi_n^{m+1,k}\dfrac{\Theta_l}{d\theta_j} \\ \left.\dfrac{\partial g_i}{\partial\varphi_j}\right|_{\varphi_j=\varphi_j^{m+1}} & = \ \alpha[L_{ij} - U_{inj}\Theta_n^{m+1,k}] \end{cases} \tag{8}$$

The computation is initiated by an estimate of the unknown dependent variables $\{\theta_j^{m+1,k}, \varphi_j^{m+1,k}\}^T$ and is updated according to $\{\theta_j^{m+1,k}+\Delta\theta_j^{m+1,k}+\varphi_j^{m+1,k}+\Delta\varphi_j^{m+1,k}\}$, where the incremental values $\{\Delta\theta_j^{m+1}, \Delta_j^{m+1}\}$ are obtained by solving the matrix equation

$$[J_{ij}^m]\left\{\begin{array}{c}\Delta\theta_j^{(m+1)} \\ \Delta\varphi_j^{(m+1)}\end{array}\right\} = -g_i^{(m+1)} \tag{9}$$

where the superscript k represents the iteration counter. Equation (8) is solved iteratively until the difference between subsequent values falls within a predetermined value of error tolerance. We refer to this model as mod-1.

2.2. Green element formulation by cubic Hermitian basis function

In mod-1, line segments (elements) have been used to discretize the problem domain and linear interpolation polynomials are applied to approximate the dependent variables and their functions within those line segments. These interpolating procedure guarantees what is known FEM speak as zero-order continuity in the sense that only the dependent variables and their functions are inter-element continuous but not their first derivatives. For the second model we employ first-order cubic Hermitian polynomials which ensures that both the dependent variables as well as their first derivatives are continuous across an element. We expect an improvement in accuracy but at a price of more tedious computation. The line integral in equation (4) is evaluated by applying the cubic Hermitian interpolation function to approximate the dependent variable and its spatial derivative

$$\theta(x,t) \approx \Omega_j(\xi)\theta(t) + \hat{\Omega}_j(\xi)\,\frac{\partial \theta_j(t)}{\partial x} = \Omega(\xi)\theta(t) + \hat{\Omega}_j(\xi)\varphi_j(t) \tag{10}$$

where Ω_j and $\hat{\Omega}_j$ are defined in terms of a local coordinate $\xi{=}\frac{(x-x_1)}{(x_2-x_1)} = \frac{(x-x_1)}{l}$ as

$$\Omega_1(\xi) = 1.0 - 3\xi^2 + 2\xi^3 \tag{11a}$$

$$\Omega_2(\xi) = 3\xi^2 - 2\xi^3 \tag{11b}$$

$$\Omega_1(\xi) = l\xi(\xi-1) \tag{11c}$$

$$\Omega_2(\xi) = l\xi(\xi-1) \tag{11d}$$

Applying the cubic Hermitian interpolation, equation (4) becomes

$$\begin{aligned} &R_{ij}\theta_j - V_{inj}\Theta_n\theta_j - \hat{V}_{inj}\left(\frac{d\Theta}{d\theta}\varphi\right)_n \theta_j + S_{inj}\psi_n\left(\frac{d\theta}{dt}\right)_j + \hat{S}_{inj}\psi_n\left(\frac{d\psi}{d\theta}\right)_j\left(\frac{d\theta}{dt}\right)_n \\ &+ L_{ij}\theta_j - \hat{V}_{inj}\Theta_n\theta_j - \check{V}_{inj}\left(\frac{d\Theta}{d\theta}\varphi\right)_n \theta_j + \hat{S}_{inj}\psi_n\left(\frac{d\theta}{dt}\right)_j + \check{S}_{inj}\psi_n\left(\frac{d\psi}{d\theta}\right)_j\left(\frac{d\varphi}{dt}\right)_n \\ &+ S_{inj}\psi_n f_j + \hat{S}_{inj}\psi_n\left(\frac{dF}{d\theta}\varphi\right)_j + \hat{S}_{inj}\left(\frac{d\psi}{d\theta}\right)_j f_n + \check{S}_{inj}\left(\frac{d\psi}{d\theta}\varphi\right)_n\left(\frac{dF}{d\theta}\varphi\right)_j = 0 \end{aligned} \tag{12}$$

Equation(12) is a nonlinear system of discrete first-order differential equations in which the element matrices have the following expressions.

$$R_{ij} = \begin{bmatrix} -1 & 1 \\ 1 & -1 \end{bmatrix} \begin{bmatrix} l_{max} & -(l+l_{max}) \\ (l+l_{max}) & -l_{max} \end{bmatrix} \tag{13a}$$

$$V_{inj} = \tfrac{1}{l}\int_0^1 G(\xi,\xi_i)\tfrac{d\Omega_n}{d\xi}\tfrac{d\Omega_j}{d\xi}d\xi \tag{13b}$$

$$\hat{V}_{inj} = \tfrac{1}{l}\int_0^1 G(\xi,\xi_i)\tfrac{d\Omega_n}{d\xi}\tfrac{d\hat{\Omega}_j}{d\xi}d\xi \tag{13c}$$

$$\check{V}_{inj} = \tfrac{1}{l}\int_0^1 G(\xi,\xi_i)\tfrac{d\hat{\Omega}_n}{d\xi}\tfrac{d\hat{\Omega}_j}{d\xi}d\xi \tag{13d}$$

$$U_{inj} = \tfrac{1}{l}\int_0^1 G(\xi,\xi_i)\Omega_n\tfrac{d\Omega_j}{d\xi}d\xi \tag{13e}$$

$$\hat{U}_{inj} = \tfrac{1}{l}\int_0^1 G(\xi,\xi_i)\Omega_n\tfrac{d\hat{\Omega}_j}{d\xi}d\xi \tag{13f}$$

$$W_{inj} = \tfrac{1}{l}\int_0^1 G(\xi,\xi_i)\hat{\Omega}_n\tfrac{d\Omega_j}{d\xi}d\xi \tag{13g}$$

$$\hat{W}_{inj} = \tfrac{1}{l}\int_0^1 G(\xi,\xi_i)\hat{\Omega}_n\tfrac{d\hat{\Omega}_j}{d\xi}d\xi \tag{13h}$$

$$S_{inj} = \tfrac{1}{l}\int_0^1 G(\xi,\xi_i)\Omega_n\Omega_j d\xi \tag{13i}$$

$$\text{(13j)} \qquad \hat{S}_{inj} = \frac{1}{l}\int_0^1 G(\xi,\xi_i)\Omega_n\hat{\Omega}_j d\xi$$

$$\text{(13k)} \qquad \check{S}_{inj} = \frac{1}{l}\int_0^1 G(\xi,\xi_i)\hat{\Omega}_n\hat{\Omega}_j d\xi$$

A two-level discretization is applied to approximate the temporal derivatives and the Picard scheme is applied to linearize the nonlinear terms to yield

$$\left\{\begin{array}{l}\alpha\left[L_{ij}\varphi_j - \hat{V}_{inj}\{\alpha\Theta_n^{(m+i,k)}+\omega\Theta_n^{(m)}\} - \overline{V}_{inj}\left\{\alpha\left(\frac{d\Theta}{d\theta}\varphi\right)_n^{(m+1,k)} + \omega\left(\frac{d\Theta}{d\theta}\varphi\right)_n^{(m)}\right\}\right] \\ +\frac{\hat{S}_{inj}}{\Delta t}\left(\alpha\psi_n^{(m+1,k)} + \omega\psi_n^{(m)}\right) + \frac{\dot{S}_{inj}}{\Delta t}\left(\alpha\left(\frac{d\psi}{d\theta}\right)_n^{(m+1,k)} + \omega\left(\frac{d\psi}{d\theta}\right)_n^{(m)}\right)\end{array}\right\}\varphi_j^{(m+1,k+1)}$$

$$\text{(14)} \quad = -\left[\begin{array}{l}\left\{\begin{array}{l}\omega\left[R_{ij}\theta_j - V_{inj}\{\alpha\Theta_n^{(m+1,k)}+\omega\Theta_n^{(m)}\} - \hat{V}_{inj}\left\{\alpha\left(\frac{d\Theta}{d\theta}\varphi\right)_n^{(m+1,k)} + \omega\left(\frac{d\Theta}{d\theta}\varphi\right)_n^{(m)}\right\}\right] \\ -\frac{S_{inj}}{\Delta t}(\alpha\Psi_n^{(m+1,k)}+\omega\psi_n^{(m)}) - \frac{\hat{S}_{inj}}{\Delta t}\left(\alpha\left(\frac{d\Psi}{d\theta}\right)_n^{(m+1,k)} + \omega\left(\frac{d\Psi}{d\theta}\right)_n^{(m)}\right)\end{array}\right\}\theta_j^{(m)} \\ +\left\{\begin{array}{l}\omega\left[L_{ij}\varphi_j - \hat{V}_{inj}\{\alpha\Theta_n^{(m+1,k)}+\omega\Theta_n^{(m)}\} - \bar{V}_{inj}\left\{\alpha\left(\frac{d\Theta}{d\theta}\varphi\right)_n^{(m+1,k)} + \omega\left(\frac{d\Theta}{d\theta}\varphi\right)_n^{(m)}\right\}\right] \\ -\frac{\hat{S}_{inj}}{\Delta t}(\alpha\Psi_n^{(m+1,k)}+\omega\psi_n^{(m)}) - \frac{\ddot{S}_{inj}}{\Delta t}\left(\alpha\left(\frac{d\Psi}{d\theta}\right)_n^{(m+1,k)} + \omega\left(\frac{d\Psi}{d\theta}\right)_n^{(m)}\right)\end{array}\right\}\varphi_j^{(m)} \\ +S_{inj}[\alpha\Psi_n^{(m+1,k)}+\omega\Psi_n^{(m)}][\alpha F_n^{(m+1,k)}+\omega F_n^{(m)}] \\ +\hat{S}_{inj}[\alpha\Psi_n^{(m+1,k)} + \omega\Psi^{(m)_n}]\left[\alpha\left(\frac{dF}{d\theta}\varphi\right)_n^{(m+1,k)} + \omega\left(\frac{dF}{d\theta}\varphi\right)_n^{(m)}\right] \\ +\hat{S}_{inj}\left[\alpha\left(\frac{d\Psi}{d\theta}\varphi\right)_n^{(m+1,k)} + \omega\left(\frac{d\Psi}{d\theta}\varphi\right)_n^{(m)}\right][\alpha F_n^{(m+1,k)}+\omega F_n^{(m)}] \\ +\ddot{S}_{inj}\left[\alpha\left(\frac{d\Psi}{d\theta}\varphi\right)_n^{(m+1,k)} + \omega\left(\frac{d\Psi}{d\theta}\varphi\right)_n^{(m)}\right]\left[\alpha\left(\frac{dF}{d\theta}\right)_n^{(m+1,k)} + \omega\left(\frac{dF}{d\theta}\right)_n^{(m)}\right]\end{array}\right]$$

where α is a temporal derivative approximation parameter which determines the level of the difference scheme. It takes a value between zero and unity. $\omega = 1-\alpha$. The superscript k shows the iteration number while $m+1$ and m denote the current(t_{m+1}) and the previous (t_m) levels. Equation (13) is solved iteratively to yield the current values of the dependent variables: $\theta_j^{m+1,k}$ and $\varphi_j^{m+1,k}$. We refer to this formulation as Mod-2.

2.3. The finite difference Newton-Richtmeyer Scheme

We adopt a model based on the finite difference Newton-Richtmeyer linearization scheme in order to compare the relative performance of the Green element formulation against one of the traditional methods. A key issue of this method which is worth mentioning is the ease with which it deals with nonlinearity and its eventual resolution of the coefficients into a tridiagonal form which enhances numerical implementation. The solution algorithm can be formally stated as:

$$\text{(15)} \quad \begin{aligned}\frac{\Delta\theta}{\Delta t} &= \frac{[D(\theta)]_{i+1/2}^j(\theta_{i+1}^j - \theta_i^j) - [D(\theta)]_{i-1/2}^j(\theta_i^j - \theta_{i-1}^j)}{\Delta x^2} \\ &+\frac{[D(\theta)]_{i+1/2}^j(\Delta\theta_{i+1}^j - \Delta\theta_i^j) - [D(\theta)]_{i-1/2}^j(\Delta\theta_i^j - \Delta\theta_{i-1}^j)}{\Delta x^2} \\ &+\frac{\left[\frac{\partial D(\theta)}{\partial\theta}\right]_{i+1/2}^j(\Delta\theta_{i+1}^{j+1} - \Delta\theta_i^{j+1})(\theta_{i+1}^j - \theta_i^j) - \left[\frac{\partial D(\theta)}{\partial\theta}\right]_{1+1/2}^j(\Delta\theta_i^{j+1} - \Delta\theta_{i-1}^{j+1})(\theta_i^j - \theta_{i-1}^j)}{2\Delta x^2}\end{aligned}$$

And any nonlinearity resulting from source, sink or reaction terms is linearized according to:

$$[F]_i^{j+1} = [F]_i^j + \frac{\partial}{\partial t}[F]\Delta t \tag{16}$$

where i and j refer to the space and time coordinates and is the immediate dependent variable . The process is executed iteratively until the difference between the old and new values falls within a prescribed error tolerance. This is third model mod-3 .

3. Numerical calculations

Examples of transient heat conduction in nonlinear materials are used to validate and compare the current models. The first example is a nonlinear heat conduction problem with a constant heat capacity but without any exact solution. The second example involves temperature dependence on both the conductivity and heat capacity in addition, it possesses a closed form solution. In the third set of calculations we shall verify the ability of the models to handle cases involving nonlinear conductivity and reaction terms.

Example 3.1 [35] involves a semi-infinite bar 20.0cm long at an initial temperature of and subjected to a temperature jump expressed by the following boundary conditions at $x = 0$

$$\begin{array}{ll} \theta = 200.0 & 0 < t \leq 10.0 \\ \theta = 100.0 & t > 100 \end{array}$$

and at $x = L : \theta = 100^0C \; t > 0$.

The thermophysical properties are for both the heat capacity and the temperature dependent thermal diffusion are given as: $D(\theta) = 2.0 + 0.01\theta$, $\rho c = 8.0$. The numerical calculations for the three models are executed using 21 grid points in a 1-D domain and a uniform time step of $\Delta t = 0.1$ in line with the parameters used in [35] in their FEM calculations. In order to enhance comparison and validation, mod-1, mod-2 and mod-3 calculations are plotted alongside the FEM solutions at time 10 and 13. Figure 1 illustrates the temperature histories predicted by the three models in comparison with that of FEM. While those of mod-1 and mod-2 are in close agreement with FEM solutions, mod-3 shows a minor deviation with the rest especially in those areas which exhibit maximum slope in the solution profile. We carried the numerical experimentation a step further by decreasing the time step ($\Delta t = 0.01$) for the three models and comparing the numerical results with those of FEM at $\Delta t = 0.1$.

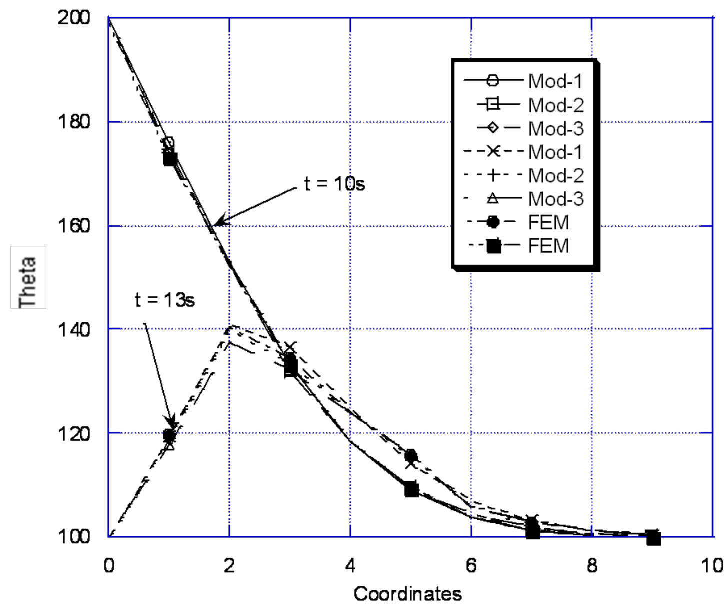

Figure 1: Temperature history predicted by the 3 models($\Delta t = 0.1$)

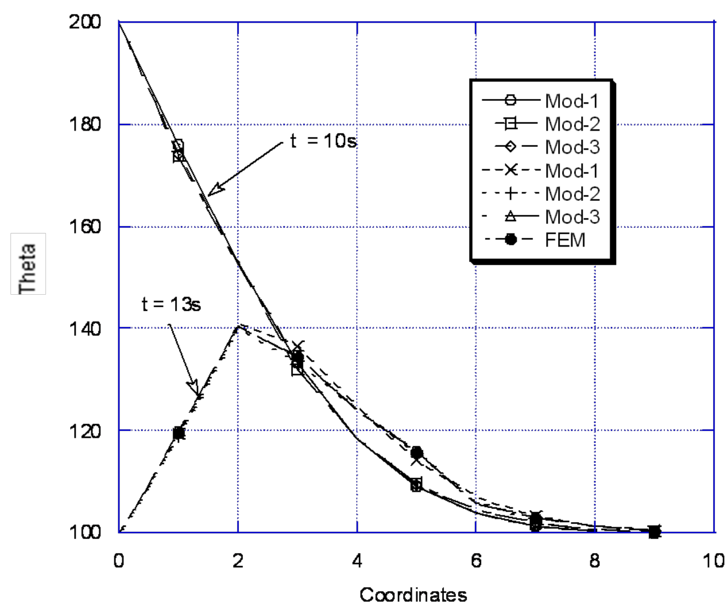

Figure 2: Temperature history predicted by the 3 models($\Delta t = 0.01$)

Figure 2 shows that while there is hardly any change in the profiles for mod-1 and mod-2, results obtained from mod-3 appear to be in closer agreement with the other profiles. These results not only validate the formulations and accuracy of the models but also confirms the higher convergence rate of the GEM models.

Example 3.2 In this example, we consider a nonlinear transient heat conduction for a 2.0 length semi-infinite bar with a constant heat input. The bar initially at a temperature of 0^0C throughout its entire length is subjected to a constant heat input $-D(\partial\theta\partial n) = 1.0$ at its left end boundary and a zero flux at the right end$(x = L)$. Both the heat capacity and thermal conductivity are expressed as $D(\theta) = \rho(\theta) = 1.0 + 0.5\theta$. The analytical solution of this problem can be found in [35] and is given as:

$$\theta(x,t) = 2\left\{\sqrt{\left[1.0 + 2.0\frac{\sqrt{t}}{\sqrt{\pi}}exp\left(\frac{-x^2}{4t}\right) - xerfc\left(\frac{x}{2\sqrt{t}}\right)\right]} - 1.0\right\}$$

Using a 0.1 length spatial elements for the problem domain and a time step of 0.5 the scalar history for mod-1, mod2 and mod-3 together with the analytical solutions are presented in Figure 3.

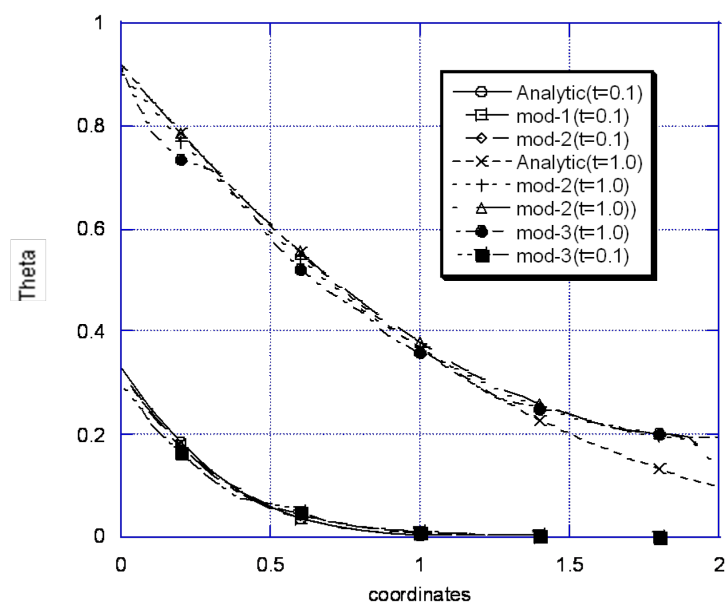

Figure 3: Comparison of analytical and numerical results at $t = 0.1$ and $t = 1.0$

The results appear to be close. However, a more detailed analysis of the error norms generated by the solutions as presented in Table 1 shows the overall superiority of mod-2 over the other two models.

Error calculation For Example 2 ($t = 0.1$)			
Models	RMs	$L_2 norm$	$L_{\inf}$ norm
Mod-1	0.566361e-02	0.2595393e-03	0.145253e-01
Mod-2	0.54185e-02	0.248309e-01	0.12457e-01
Mod-3	0.50504e-02	0.229876e-01	0.175463e-01
Error calculation For Example 2 ($t = 0.5$)			
Models	RMs	$L_2 norm$	$L_{\inf}$ norm
Mod-1	0.964653e-02	0.513488e-01	0.233718e-01
Mod-2	0.696495e-02	0.319174e-01	0.180562e-01
Mod-3	0.816381e-02	0.665743e-01	0.300975e-01
Error calculation For Example 2 ($t = 1$)			
Models	RMs	$L_2 norm$	$L_{\inf}$ norm
Mod-1	0.370983e-01	0.170000e+00	0.934392e-01
Mod-2	0.358708e-01	0.164381e+00	0.911992e-01
Mod-3	0.401325e-01	0.199785e+00	1.00875e-01

Table 1: Comparison of errors for the three models

Table 2 shows the temperature as a function of time at the left end boundary brought about by a constant heat supply. Mod-2 displays a marginal superiority over the other models followed by mod-1. This is an indication of the ability of the GEM technique to handle nonlinear boundary conditions in a straightforward manner.

Example 3.3 Our aim here is to check how the models can correctly represent the effects of nonlinear source terms on the scalar profile of a heat conduction process involving a thermally dependent conductivity term or variable properties [36]. Let us consider the following problem for the governing differential equation as represented by equation (1):

$$\begin{aligned} D(\theta) &= \theta & F(x,t,\theta) &= \theta^2 \\ \theta(0,t) &= 1 & \theta(1,t) &= 0.0 \\ \theta(x,0) &= 0.0 \end{aligned}$$

The steady state solution of the above problem is given as:

$$\theta(x,t) = \left\{cosh[x\sqrt{2}] - coth[\sqrt{2}]sinh[x\sqrt{2}]\right\}^{1/2}$$

Table 3 shows that the numerical results for all the models are almost the same for this problem at steady state. Whatever gains made by Mod-2 because of its Hermite interpolation procedure are hardly noticeable at steady state.

Temperature at the left end boundary ($x = 0$)				
Time	Analytical	mod-1	mod-2	mod-3
0.05	0.2381e+00	0.2523e+00	0.2275e+00	0.2514e+00
0.10	0.3297e+00	0.3145e+00	0.3217e+00	0.3154e+00
0.15	0.3975e+00	0.3902e+00	0.3920e+00	0.3892e+00
0.20	0.4533e+00	0.4458e+00	0.4449e+00	0.4417e+00
0.25	0.5014e+00	0.4934e+00	0.4946e+00	0.4891e+00
0.30	0.5440e+00	0.5355e+00	0.53272e+00	0.5318e+00
0.35	0.5827e+00	0.5734e+00	0.5763e+00	0.5694e+00
0.40	0.6181e+00	0.6181e+00	0.6181e+00	0.6111e+00
0.45	0.6510e+00	0.6402e+00	0.6452e+00	0.6382e+00
0.50	0.6817e+00	0.6701e+00	0.6761e+00	0.6681e+00
0.55	0.7106e+00	0.6983e+00	0.7052e+00	0.6914e+00
0.60	0.7379e+00	0.7249e+00	0.7328e+00	0.7209e+00
0.65	0.7369e+00	0.7504e+00	0.7590e+00	0.7484e+00
0.70	0.7886e+00	0.7746e+00	0.7840e+00	0.7703e+00
0.75	0.8123e+00	0.7979e+00	0.8080e+00	0.7935e+00
0.80	0.8350e+00	0.8202e+00	0.8322e+00	0.7982e+00
0.85	0.8568e+00	0.8418e+00	0.8551e+00	0.8412e+00
0.90	0.8778e+00	0.8627e+00	0.8771e+00	0.8673e+00
0.95	0.8981e+00	0.8830e+00	0.8983e+00	0.8801e+00
1.00	0.9178e+00	0.9027e+00	0.8983e+00	0.8927e+00

Table 2: Temperature as a function of time at the left boundary

Numerical and analytic results at steady state				
Coordinate	Analytical	mod-1	mod-2	mod-3
0.1	0.9219e+00	0.9220e+00	0.9219e+00	0.9221e+00
0.2	0.8467e+00	0.8465e+00	0.8465e+00	0.8471e+00
0.3	0.7735e+00	0.7735e+00	0.7735e+00	0.7742e+00
0.4	0.7013e+00	0.6994e+00	0.7016e+00	0.7022e+00
0.5	0.6287e+00	0.6282e+00	0.6285e+00	0.6298e+00
0.6	0.5539e+00	0.5528e+00	0.5538e+00	0.5551e+00
0.7	0.4739e+00	0.4732e+00	0.4736e+00	0.4735e+00
0.8	0.3835e+00	0.3832e+00	0.3835e+00	0.3849e+00
0.9	0.2697e+00	0.2695e+00	0.2695e+00	0.2708e+00

Table 3: Comparison of numerical and analytic solutions at steady state

Since all the models converge to the right results at steady state, we took a closer look at the scalar evolution of all the models at different times figure 4 by allowing the source term to vary from linear, quadratic and cubic.
It is noticeable here that despite the power law variation of the source terms, the overall temperature approaches steady state at a relatively fast rate. This is

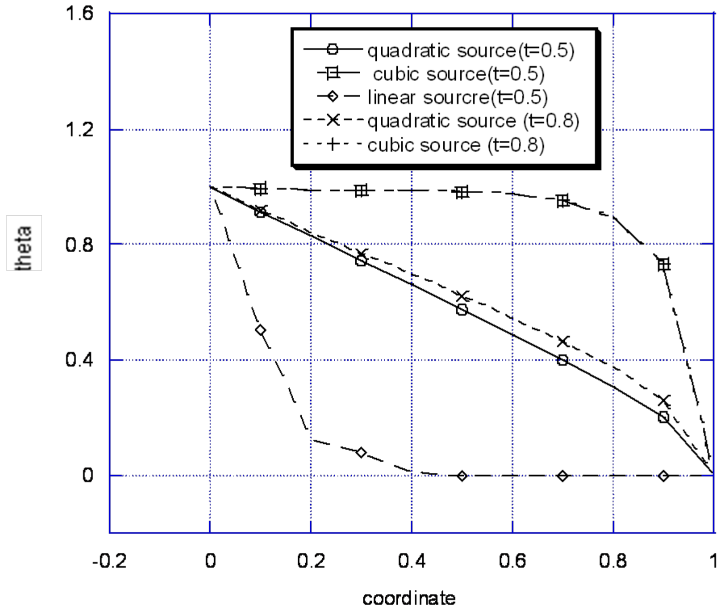

Figure 4: Solution Profiles at different times

attributed to the nonlinearity of this problem caused by its temperature-dependent thermophysical properties. As a result, heat is prevented from being conducted as rapidly as would have been the case if it were a for a constant property problem.

4. Conclusion

In this paper, the usefulness of using a one-dimensional hybrid boundary element method has been presented. Three models have been created and one of them uses a cubic hermitian formulation to interpolate the dependent variables. The relative gains made by this more complicated formulation have been shown to be marginal. This may have a bearing to the class of problems addressed in this work. It may prove to be the case, that when the steepness of the scalar variable is not so profound, that BEM hermitian interpolation may not be the direction to go. At the same time this work raises the issues involved in formulating robust one-dimensional boundary element algorithms that can straightforwardly handle problems that have continuously raised concerns to the BEM community especially those that are transient, heterogeneous, and nonlinear. The usual practice of using two-dimensional formulation to solve problems that are typically one-dimensional by imposing no-flux conditions at the boundaries are issues that need be addressed as relevant details concerning both the physics of the problem and its application stand the risk of being obfuscated. My current work points in this direction.

Acknowledgement. I will like to thank my colleagues at the African Institute of Mathematical Sciences (AIMS) at Muizenburg South Africa for giving access to their facilities.

References

[1] Cho Lik Chan, *A local iteration scheme for nonlinear two-dimensional steady-state heat conduction*, a BEM approach Applied Math Mod., 17 (1993), 650-657.

[2] Bialecki, R., Nowak, A.J., *Boundary value problems in heat conduction with nonlinear material and nonlinear boundary conditions*, Applied Math Mod., 5 (1981), 417.

[3] Bialecki, R., Nahlik, R., *Solving nonlinear steady-state potential problems in inhomogeneous bodies using boundary-element method*, Numerical Heat Transfer, B 6 (1989), 79.

[4] Mukherjee, S., Morjaria, M., *On the efficiency and accuracy of the boundary element method and finite element method*, Int. Journal of Numerical Engineering, 50 (1982), 515.

[5] Mohammadi, M., Hematiyan, M.R., Marin, L., *Boundary element analysis of nonlinear transient heat conduction problems involving non-homogeneous and nonlinear heat sources using time dependent fundamental solutions*, Engineering Analysis with Boundary Elements, 34 (2010), 655-665.

[6] Branco, J.B., Ferreira, J.A., *Boundary element analysis of nonlinear transient heat conduction problems involving non-homo generous and non-linear heat sources using time-dependent fundamental solutions*, Applied Numerical Mathematics, 57 (2007), 89-102.

[7] Sladek, J., Sladek, V., Zang, Ch., *A local BIEM for analysis of transient heat conduction with nonlinear source terms in FGMs; Engnr*, Anal. Boundary Elements, 28 (2004), 1-11.

[8] Tanaka, M., Matsumoto, T., Suda, Y., *A dual reciprocity boundary element method applied to the steady state heat conduction problem of functionally graded materials*, Electron J. Boundary Elem., 1 (2002), 128-135.

[9] Werner-Juszczuk, A.J., Sorko, S.A., *Application of boundary element method to the solution of transient heat conduction*, Acta Mechanica et Automatica, 6 (2012), 67-74.

[10] Bialecki, R.A., Jurga, P., Kuhn, G., *Dual reciprocity BEM without matrix inversion for transient heat conduction*, Engineering Analysis with Boundary Elements, 26 (2002), 227-236.

[11] Erhat, K., Divo, E., Kassab, A.J., *A parallel domain decomposition boundary element approach for the solution of large-scale transient heat conduction problems*, Engineering Analysis with Boundary Elements, 30 (2006), 553-563.

[12] Johanson, B.T., Lesnic, D., *A method of fundamental solutions for transient heat conduction*, Engineering Analysis with Boundary Elements, 32 (2008), 697-703.

[13] Johanson, T., Lesnic, D., *A method of fundamental solutions for transient heat conduction in layered materials*, Engineering Analysis with Boundary Elements, 33 (2008), 697-703.

[14] Tanaka, M., Takakuwa, S., Matsumoto, T., *A time stepping DRBEM for transient heat conduction in anisotropic solids*, Engineering Analysis with Boundary Elements, 32 (2008), 1046-1053.

[15] Kikuta, M., Togoh, H., Tanaka, M., *Boundary element analysis of nonlinear transient heat conduction problems*, Computer Methods in Applied Mechanics and Engineering, 62 (1987), 321-329.

[16] Pasqueti, R., Caruso, A., *Boundary element approach for transient and nonlinear thermal diffusion*, Numerical Heat Transfer, Part B 17 (1990), 83-89.

[17] Ochiai, Y., Kitayama, Y., *Three-dimensional unsteady heat conduction analysis by triple-reciprocity boundary element method*, Engineering Analysis with Boundary Elements, 33 (6) (2009), 789-795.

[18] Ochiai, Y., Sladek, V., Sladek, J., *Transient heat conduction analysis by triple reciprocity boundary element method*, Engineering Analysis with Boundary Element, 30 (3) (2006), 194-204.

[19] Yang, K., Gao, X.-W., *Radial integration BEM for transient heat conduction problems*, Engineering Analysis with Boundary Elements, 34 (2010), 557-563.

[20] Taigbenu, A.E., *The Green element method*, International Journal for Numerical methods in Engineering, 38 (1995), 2241-2263.

[21] Taigbenu, A.E., *The Green element method*, Kluwer Academic Publishers, Boston, Dordrecht, London, 1999.

[22] Taigbenu, A.E., Sada, E., *A Green element model for variably saturated groundwater flow*, Proc. International Conference on Computational Methods in Water Resources, Denver CO; June 1992, 1219-227.

[23] Onyejekwe, O.O., *A Green element application to the diffusion equation Proceedings 35th heat transfer and fluid mechanics*, Institute, California State University, Sacramento California, 1990, 75-90.

[24] Taigbenu, A.E., Onyejekwe, O.O., *Green function-based integral approached to nonlinear transient boundary-value problems* (II), Applied Math. Modelling, 22 (1998), 241-253.

[25] Onyejekwe, O.O., *Green element description of mass transfer in reacting systems*, Numerical Heat Transfer., B 30 (1996), 483-498.

[26] Taigbenu, A.E., *The flux-correct Green element formulation for linear, nonlinear heat transport in heterogeneous media*, Engineering Analysis for Boundary Element Method, 32 (2008), 52-63.

[27] Onyejekwe, O.O., *Green element procedures accompanied by nonlinear reaction*, International Journal of Thermal Sciences, 42 (2003), 813-820.

[28] Onyejekwe, O.O., *Subsurface drainage of sloping lands*, Engineering Analysis with Boundary Elements, 23 (1999), 619-624.

[29] Archer, R., *Continuous solutions from Green element method using Overhausser elements*, App. Num. Maths., 56 (2006), 222-229.

[30] Taigbenu, A.E., Onyejekwe, O.O., *Green element simulations of transient nonlinear unsaturated flow equation*, Applied Math. Medelling, 19 (1995), 675-684.

[31] Onyejekwe, O.O., *Boundary integral procedures for unsaturated flow problems*, Transport in Porous Media, 31 (1998), 313-330.

[32] Onyejekwe, O.O., *Solution of nonlinear transient conduction equation by a modified boundary integral procedure*, Int. Communications Heat and mass Transfer, 25 (1998), 1189-2002.

[33] Taigbenu, A.E., Onyejekwe, O.O., *A mixed Green element formulation for transient Burgers' equation*, International Journal for Numerical methods in Fluids, 24 (1997), 563-578.

[34] Onyejekwe, O.O., *A Green element treatment of isothermal flow with second order reaction*, Int. Communication Heat and Mass Transfer, 97 (1997), 251-264.

[35] Segal, A., Praagman, N., *A fast implementation of explicit time-stepping algorithms with the finite element method for a class of nonlinear evolution problems*, Int. Jnl. Num. Mthd. Engnr., 14 (1979), 1461-1476.

[36] Moisheki, R.J., Makinde, O.D., *Computational Modelling and similarity reduction of equations for transient fluid flow and heat transfer with variable properties*, Advances in Mechanical Engineering, 2013 (2013), Article ID 983962, 8 pages http://dx.doi.org/10.1155/2013/983962.

Accepted: 30.01.2015